



Effect of tool rotational speed on friction stir welding of polymer using self-heated tool

Rahul Kanti Nath¹ · Pabitra Maji¹ · John Deb Barma¹

Received: 9 January 2022 / Accepted: 14 February 2022 / Published online: 28 February 2022
© The Author(s) under exclusive licence to German Academic Society for Production Engineering (WGP) 2022

Abstract

With the growing development in industrial applications of commodity plastics, demand for quick and reliable welding methods has increased. Friction stir welding (FSW), a newly developed technique, is widely used for joining polymer materials. In the present study, friction stir welding is carried out on a 3 mm polypropylene (PP) sheet by a novel self-Heated FSW tool in which external force creates additional frictional heat. Tool rotational speed is varied with fixed tool traverse speed and tool tilt angle. This investigation is aimed to study the forces and torque engendered on the tool during the welding and their effect on the joint quality. The microstructural morphologies of the weldments are analysed by two different microscopes such as cross-polarized light microscope and scanning electron microscope. To evaluate the mechanical characteristics of the welded joints; microhardness test, tensile test and flexural tests are performed. The tool forces and spindle torque decreased with the increment of tool rotational speed owing to greater softening of the material. This reduced forces and torque leading to better mixing of materials at the interface of the butt joint. Though the proper bonding is achieved by this novel tool, a few micropores are observed in the stir zones. Although, with the increase of tool rpm, the microhardness is reduced due to a high-level at material softening, owing to better material mixing at higher rpm, tensile strength and flexure strength are increased with rise of tool rpm up to 1600 rpm.

Keywords Friction stir welding · Polypropylene · Self-heated FSW tool · Microhardness · Tensile strength

1 Introduction

Recently, FSW is increasingly attracting consideration in the aerospace and automobile industries as an effective and promising joining technique of thermoplastics [1–3]. The advantages of FSW include environmentally friendly processes, energy efficiency, and high joint strength with excellent weld quality [4]. Over the years, several characteristics of FSW of polymer such as the response of the process parameters [5, 6] and influence of the tool profile [7–9] on the mechanical properties have been studied.

The major difficulty in FSW of polymer is the typical characteristics of polymer such as low thermal conductivity, low frictional coefficient with tool material, variable melting temperature etc. Due to this, the range of process parameter for suitable heat is very minimal. In FSW process, tool rpm and

plunge pressure directly influence the generation of heat at weld zone [10]. In case of polymer welding, higher level of tool rpm causes high level of heat generation along with material distortion from the weld zone [7]. For welding of thick polymeric plate, joining can be achieved by the higher level of plunging depth to supply the adequate amount of frictional heat [11, 12]. Whereas, this technique is not feasible for thin polymeric sheet as the excessive plunge depth may cause collision of the tool pin with back supporting plate. Owing to the different behaviour of polymer material at the time FSW as compared to metals, it is established that a conventional FSW tool may not be suitable for welding thin sheet polymeric materials [13]. In order to overcome these difficulties, various special FSW tools for polymeric material have been introduced by various researchers. Bagheri et al. [14] have developed a tool with electric heater assisted heated shoe called hot shoe which act as a stationary shoulder and allows supplying additional heat during the joining of acrylonitrile butadiene styrene (ABS) sheet. They have found that higher level of shoe temperature i.e., 100 °C, can produce better weld quality and joint strength. Banjare et al. [15] have enhanced

✉ Rahul Kanti Nath
riserrahul@gmail.com

¹ Department of Mechanical Engineering, NIT Agartala, Agartala, Tripura (W) 799046, India

tool flexibility by putting an electric heater centre in a conventional FSW tool after modifying the tool design. Mendes et al. [16] have introduced robotic FSW for 6 mm thick ABS plate and they have obtained maximum joint efficiency of 75.5% at tool temperature of 115 °C. Azarsa et al. [17] have used similar tool to join thick (10 mm) high-density polyethylene (HDPE) plates. With shoe temperature of 110 °C, they have obtained ultimate relative flexural strength of 95.69%. To eliminate the root defect, Pirizadeh et al. [18] have developed a tool namely "self-reacting tool" for ABS sheets. The tool has two shoulders, one touches upper surface and another at lower surface of the workpiece, and simple and convex pin profile. Comparing with two pin profile they have found that convex pin profile offers better mechanical performance. Vijendra and Sharma [19] have performed hybrid process of induction heated tool-assisted FSW for joining of a 5 mm thick HDPE plate. Where induction heater has been used as a secondary heat source during the welding. Eslami et al. [20] have performed overlap joining of two dissimilar polymers PP and Polystyrene (PS) using a newly developed stationary shoulder FSW tool. They have found that the stationary shoulder made of Teflon polymeric material can produce stronger welds with good surface quality compared to wood, brass and aluminium shoulders. Mochani et al. [21] have developed heat-assisted FSW tool in which they have used controllable hot air gun as supplementary heating source. They have performed butt welding of 4 mm PP sheets with 130 °C, 150 °C and 170 °C tool temperature. Among these three different tool temperatures they have found that tool temperature 150 °C can offer better mechanical attributes in terms of strength and elongation.

From literature, it is evident that FSW of polymer, especially of thin polymer sheet may lead to various defects and therefore, attempts have been made to modify the tool design with additional heating arrangement. Although the tools with additional heater enables excellent joining, the major limitation of these tools are the requirement of extra electric supply and higher shop floor occupancy. Therefore, in the current investigation, a self-heated FSW tool is used to weld 3 mm PP sheets. The tool can provide supplementary heat to the weld material without the additional electrical requirements. During the welding tool, the rotational speed is varied at different level to study the effect on different tool pin forces and weld quality. Also, to study the mechanical attributes of the welds, microhardness test, tensile test and flexural tests are performed.

2 Experimental procedures

In the present study 3 mm PP sheets are with dimensions of 100 mm length and 60 mm width used as weld material. The properties of the PP are presented in Table 1. PP is one of the most important commodity thermoplastics having good

corrosion resistance, excellent design freedom, and easy manufacturing process [22–24].

Joining are performed in butt configuration with different parametric condition. Figure 1 shows the major four different stages of FSW butt welding, which are tool plunging, dwelling, welding and tool retraction. The rotating tool plunges the weld materials during the plunge phase by moving in axial direction. The tool's downward motion is halted as soon as the tool shoulder makes contact with the workpiece surface. The tool is maintained in a suggested position for a period of time after the plunging phase to allow the material to warm up, which is known as the dwell phase. The rotating tool starts moving ahead along the joint line during the welding phase. When the welding is completed, the tool is quickly lifted higher from the weld seam to the specified location, which is known as the tool retraction phase. The nomenclature of the welding and tool are shown in Fig. 2. The self-heated FSW tool is designed in such a manner where frictional shoe and tool shoulder create additional frictional heat during the welding. The frictional shoes are connected to the loading unit through a brake cable. Depending upon the requirement, the supply of additional heat can be controlled by varying the load on frictional shoe. The tool has 3 mm and 12 mm pin diameter and shoulder diameter respectively. Moreover, the 2.8 mm long cylindrical pin is right-hand threaded with 0.8 mm thread pitch. The detailed description of the tool is mentioned in previous work [25]. The experiments are performed in a fully automatic 3 t FSW machine (make: ETA Technology in Bengaluru, India) loaded with strain gauge-based load cell to measure forces and torque experienced by the tool during the welding as shown in Fig. 3. With an infinite variable, the machine spindle has a maximum rotating speed of 3000 rpm. At 1650 rpm, it can produce 86.4 Nm of torque. The plunge load is applied by a hydraulic actuator with a maximum loading capacity of 30 kN. The longitudinal motion machine bed is driven by a servo motor with a 10kN load capability. With 1° constant tool tilt angle and 0.5 kgf applied frictional shoe pressure, the tool rotational speed is varied as 1400, 1500, 1600 and 1700 rpm in the clockwise direction. Throughout the experiment, the welding speed remained constant at 0.3 mm/s. After performing

Table 1 Material specification [1]

Material	Density (kg/m ³)	Thermal conductivity (W/mK)	Melting range (°C)	Tensile Strength (MPa)	Flexural strength (MPa)
Polypropylene (PP)	908	0.17–0.22	150–162	22.59	40

Fig. 1 Schematic representation of main phases involve in FSW

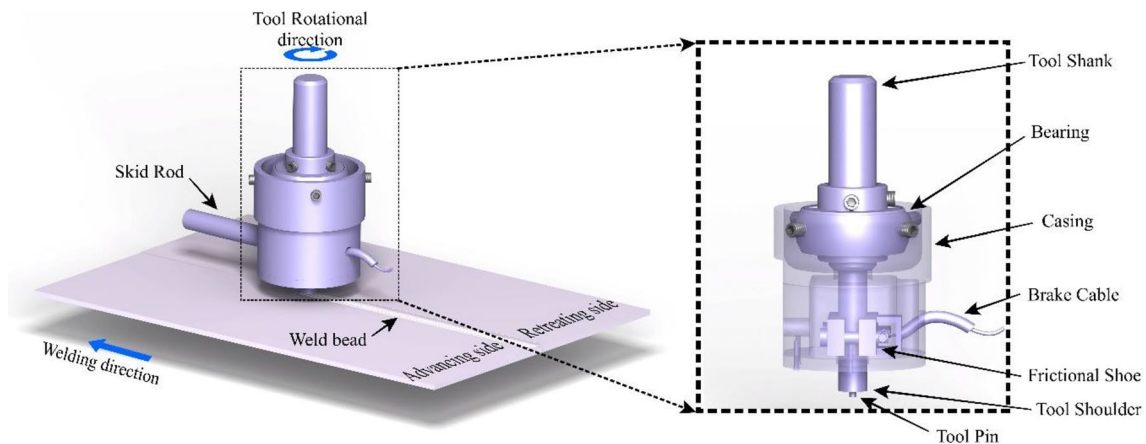
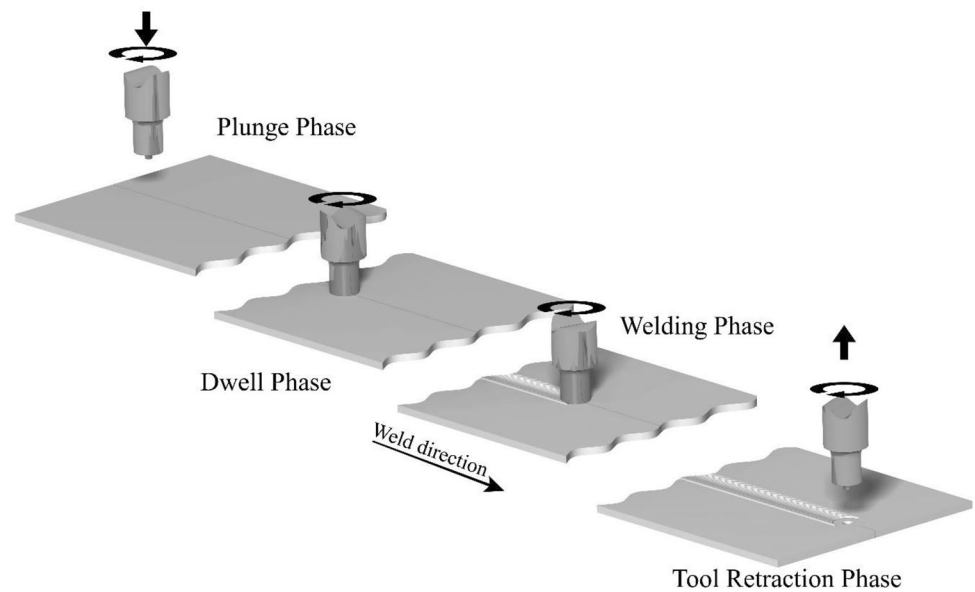


Fig. 2 Schematic of self-heated FSW process

the joining, weld specimens are prepared for the joint quality evolution. Strain gauge-based load cells were used to measure spindle torque and unique forces, such as Z-force (axial force) and X-force (transverse force), during welding. One load cell was connected to the spindle head for measuring spindle torque and Z-force, while the other was connected to the auxiliary slide for measuring X-force. For data feedback, these load cells were linked to a PLC system, and data was gathered using NI LabVIEW software. The graphs were created using the 'Origin' graphing tool after extracting data from the system. The graphs show the time-dependent connection between torque, axial force and transverse force. In this article, the average of the various forces and torque obtained during welding time are reported and their variation is plotted against the tool

rotational speed. For morphology characterization specimens are prepared according to the ASTM E 2015-04 standard [26]. To understand the effect of different tool rotation on structural changes at the stir zone, differential scanning calorimetry (DSC) analysis are performed. A load of 25 gf is applied for 10 s to measure Vickers microhardness of the weld specimens. Microhardness values are taken at 0.5 mm distance in centre line (transverse to weld direction) of the sheet to estimate the distribution over the welded specimens. ASTM D638-14 standard [27] is followed to prepare tensile test samples to determine the joint efficiency of the weld joint. Tensile tests are carried out with a constant crosshead speed of 0.5 mm/min on an Instron 8801 machine at room temperature (~ 305.15 K). Flexural tests are accomplished according to the ASTM

Fig. 3 Experimental setup for FSW process



D790-17 standard [28]. In three-point flexural tests for joint, the joint root is in tension.

3 Result and discussion

3.1 Fluctuation of spindle torque and forces on the Self-heated FSW tool

Spindle torque is the material's response to tool rotation during the welding. From Fig. 4a it is detected that the average spindle torque value decreases with the increase of tool rotational speed. It is due to minimum heat generation at low tool rpm comparing with the high tool rotational

speed [25]. The resisting forces offered by the weld material to tool movement can be measured in two ways, one is axial force (Z-force) and another is transverse force (X-force). The variation of average axial force and average transverse force with tool rotational speed are presented in Fig. 4b, c. It can be realised from the graph; the average axial force and average transverse force decreases with the increase of tool rpm. As tool rpm increases the heat generation at the tool-frictional shoe interface and tool material interface increase. Combination of both the heat sources allows the material become softer at higher rpm. As a result, reduction in spindle torque and forces experienced by the tool during interaction of tool probe and weld material can be observed at high rpm.

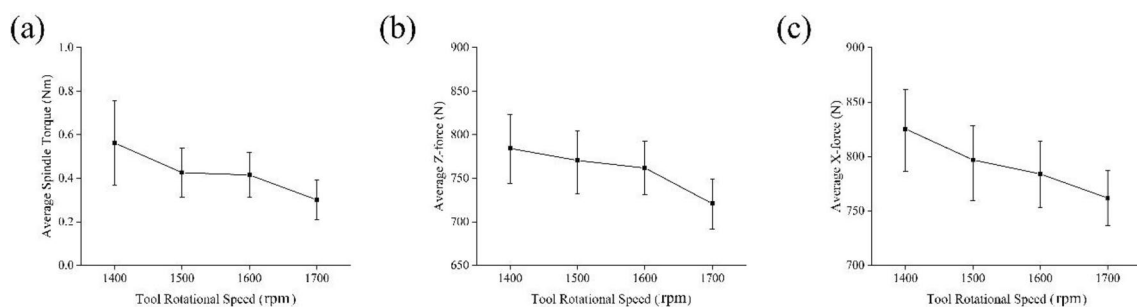


Fig. 4 Fluctuation of average **a** spindle torque, **b** axial force and **c** transverse force with tool rotational speed

3.2 Microstructural characterization of welded joints

The macrographic and micrographic analysis are carried out on the joints cross-sections of the weld zone and is revealed in Fig. 5. From Fig. 5a, b it is observed that weldment produced with tool rotation speed of 1400 rpm and 1500 rpm have micro-voids (shown in arrows) at stir zone. It is due to lack of sufficient heat generation during low tool rotational speed. This results in improper material softening and consequently leading to chip formation and irregular material flow. Due to this, the chips in form of solid particles are trapped under the stir zone. The semi-solid material flow is not able to entirely wrap the uneven solid particles. Therefore, micro-voids are formed. Whereas, with high tool rotational speed, the tool can supply an adequate amount of heat to the weld material. Thereby, the stir zone (SZ) becomes more soften compering with the SZ of the lower tool rpm. This permits the weld material at the SZ to flow uniformly without forming any micro-voids for high tool rpm as seen in Fig. 5c, d. Moreover, the thermal history encountered during manufacturing processes has a significant impact on the degree of crystallinity in polymers. The crystallinity of the stir zone deteriorates as the tool rpm increases, as seen in Fig. 6. This is because the heat generated at 1700 rpm is much higher than at lower tool rpms. The crystalline and amorphous chain structures deteriorate due to the increased heat generated by the greater tool rotating speed. As a result, a faster rotational speed causes more material softening at the stir zone, and a higher melt temperature may cause crystallisation to be delayed. Similar crystallization kinetics were also found by Nieh and Lee [29] during the hot plate welding of polypropylene material.

3.3 Microhardness

Variation of microhardness distributions at the weld zone with different tool rotational speed are represented in

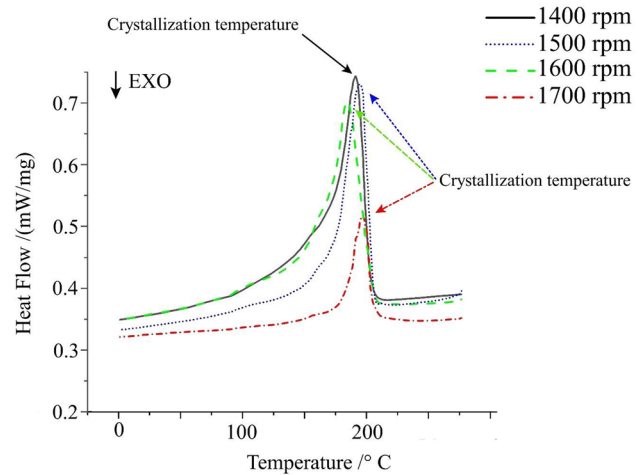


Fig. 6 DSC curves representing exothermic peak of stir zone welded with 1400 rpm, 1500 rpm, 1600 rpm and 1700 rpm

Fig. 7. It is observed that the microhardness value at the SZ in both the advancing side (AS) and retreating side (RS) decreases for all the welded specimens than the as-received PP. The microhardness values at the SZ are minimum for the weld produced with the highest tool rpm. Similar behaviour of microhardness variation is observed by Nath et al. [30] during the joining of 6 mm PP plates. The reduction of microhardness can be explained by change of crystallinity or molecular weight in the weld material by the stirring action of the tool [31]. The stirring action induces chopping of molecular chains which reduces the melt viscosity. Therefore, the material flow is stimulated. Moreover, the frictional heat produced by the tool significantly controls the smashing of molecular chains [32]. Furthermore, the heat at SZ causes deterioration of material crystallinity at the weld zone [33]. At high tool rotational speed, both the stirring action and heat generation are high. Hence, the softening of material at the SZ at higher rotational speed is observed.

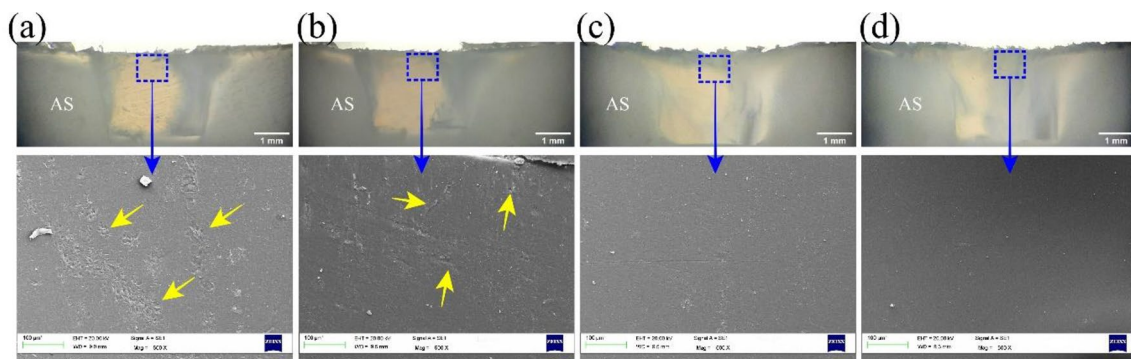


Fig. 5 Microstructural morphologies of weld for specimen join with a 1400 rpm, b 1500 rpm, c 1600 rpm and d 1700 rpm

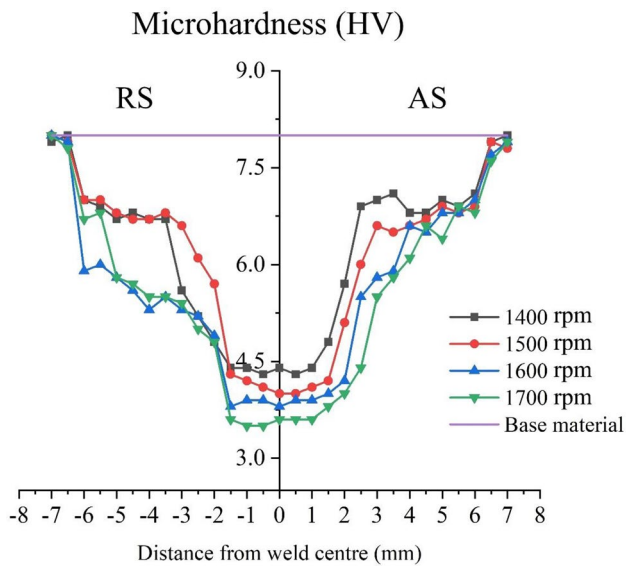
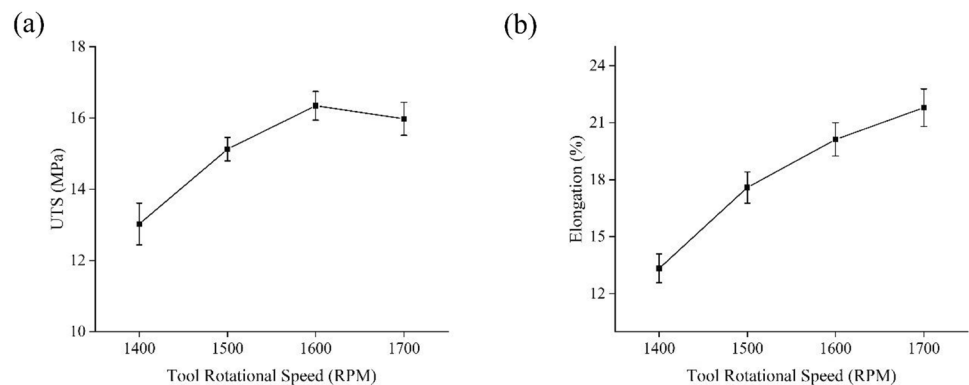


Fig. 7 Microhardness distribution of weld specimens with different tool rotational speed

3.4 Tensile strength and flexural strength

The effect of tool rotational speed on joint strength is presented in Fig. 8a. It is seen that the ultimate tensile strength improves with an increase of tool rpm up to 1600 rpm. The weld joint produced by tool speed of 1400 and 1500 rpm have defects in the weld zone (Fig. 5a, b) which causes reduction in the strength as well as in % of elongation (Fig. 6b). It can be observed that with tool rotational speed of 1600 rpm exhibits maximum joint efficiency (~16.35 MPa) of around 72.37% to the base material. It is due to the greater level of softening at the SZ which leads to the uniform material flow and defect-free stir zone [34]. Further increment in tool rotational speed yields higher level of heat generation at the SZ resulting in proper plasticization of material and void-free stir zone. However, simultaneously the higher heat at the SZ causes structural changes of material in form of reduction in crystallinity [35]. Therefore,

Fig. 8 Alteration of **a** ultimate tensile strength and **b** % elongation of welded specimens with tool rpm



decline in the joint strength ~15.98 MPa at the high level of tool rpm (1700 rpm) is observed.

The SEM images of fractured surfaces by tensile loading are illustrated in Fig. 9. The presence of fibrillar structure at the fracture surface (Fig. 9) is clear evidence of ductile fracture mode in the welded specimens. Also, the size of the fibrillar indicates the percentage of elongation of the joint. Tool rpm of 1700 rpm results in higher elongation as observed in Fig. 8b. It is due to high level of softening of the SZ owing to reduced crystallinity (Fig. 6). Also, from Fig. 9d it is seen that the fibrillar in weld at 1700 rpm are stretched more than the other joints which indicates higher elongation of the material before rupture.

In order to analyse the flexural behaviour of the weld joints, the flexural strength with different tool rpm is shown in Fig. 10. It can be noticed that for tool rpm of 1600 rpm, welds show higher flexural strength related to the other parametric condition. The maximum relative flexural strength of about 85% of the base material is reached for the weld specimen produced with tool rpm of 1600 rpm. During the double-sided welding of 6 mm PP sheets, Nath et al. [30] achieve a maximum relative flexural strength of 78.49%. Further increment of tool rotational speed leads to drop in hardness value (Fig. 7) resulting changes in mechanical properties and consequently decline in flexural behaviour.

4 Conclusions

A new tool design for thermoplastic material FSW is established and successfully used for welding of polypropylene sheets. The consequence of the tool rotational speed on the weld joints are studied. The tool rpm plays a critical role in the weld quality during the FSW process. The average spindle torque and tool forces decreases with the increase of tool rotational speed. It appears that weldment produces with low tool rpm causes a defect in the SZ due to lack of heat generated at the interface of tool and workpiece. This is overcome with the improvement in tool rpm as higher rotational speed yields uniform

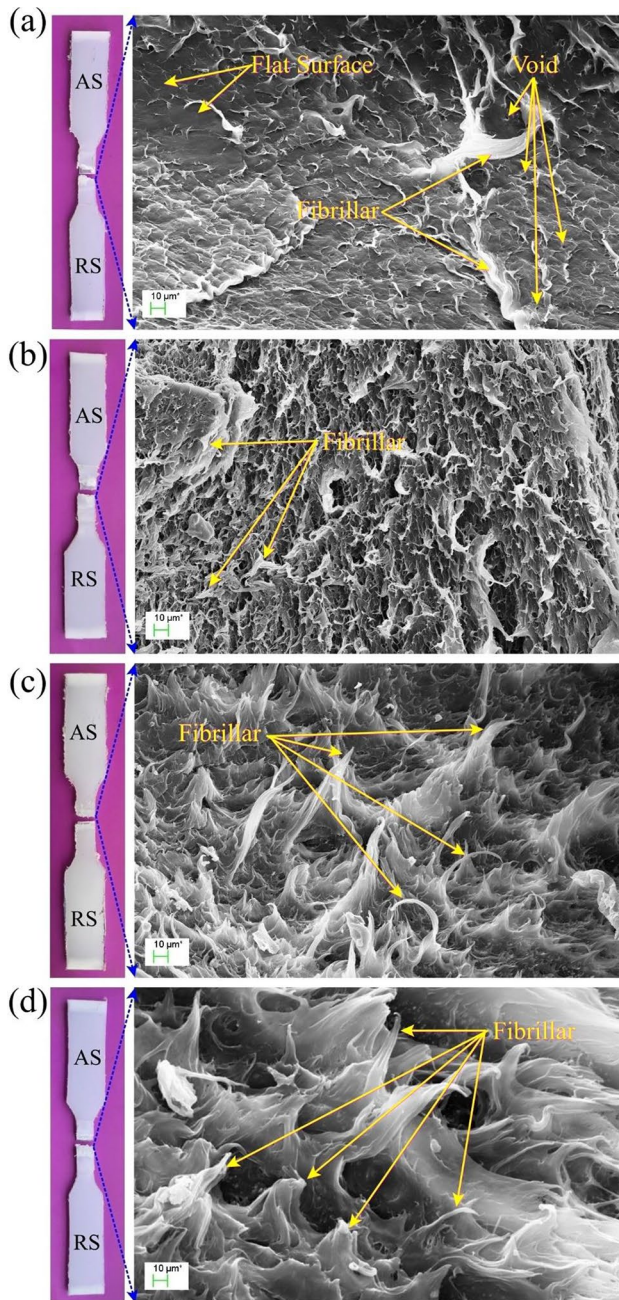


Fig. 9 SEM fractography of fractured surfaces for specimen welded with **a** 1400 rpm, **b** 1500 rpm, **c** 1600 rpm and **d** 1700 rpm

material flow. Microhardness, Tensile and flexural strength are considered as mechanical ability of the weld joint in this investigation. While the tool rpm increases microhardness at the SZ decreases. Fractography of the SEM image revealed that all fracture occurred at ductile mode of failure. According to the results obtained, tool rotational speed of 1600 rpm is able to offer the highest tensile as well as flexural strength.

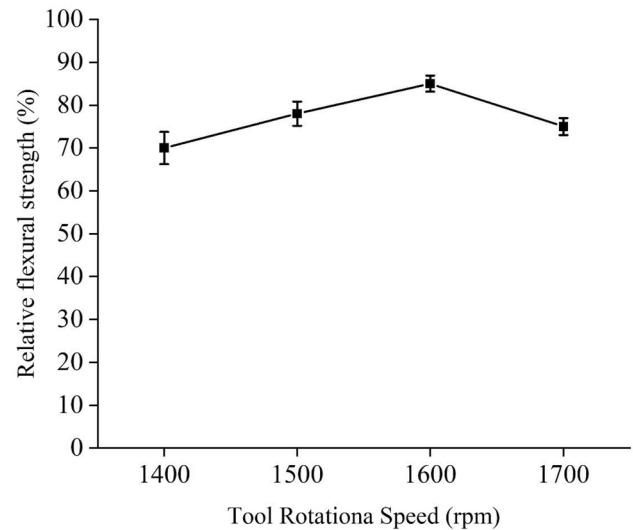


Fig. 10 Variation of relative flexural strength with tool rotational speed

Authors contributions Conceptualization, Investigation, Formal analysis and writing original draft was done by RKN. Visualization and Writing—Review & Editing was done by PM. JDB was supervising the entire work. All authors read and approved the final manuscript.

Funding Not applicable.

Availability of data and materials Data and materials associated in the article cannot be shared at this time as it a part of ongoing research work.

Declarations

Conflict of interests The authors declare that they have no competing interests.

Ethical approval Not applicable.

Consent to participate Not applicable.

Consent to publish Not applicable.

References

- Xue Y, Zhao H, Zhang Y et al (2021) Design and multi-objective optimization of the bumper beams prepared in long glass fiber-reinforced polypropylene. *Polym Compos.* <https://doi.org/10.1002/pc.26026>
- Kah P, Suoranta R, Martikainen J, Magnus C (2014) Techniques for joining dissimilar materials: metals and polymers. *Rev Adv Mater Sci* 36:152–164
- Raithel TST (2015) *Kunststoffe International*. Lightweight Innov 2015:71–73
- Nath RK, Maji P, Barma JD (2019) Development of a Self-Heated Friction Stir Welding tool for welding of polypropylene sheets.

- J Braz Soc Mech Sci Eng 41:1–13. <https://doi.org/10.1007/s40430-019-2059-2>
5. Eslami S, de Figueiredo MAV, Tavares PJ, Moreira PMGP (2018) Parameter optimisation of friction stir welded dissimilar polymers joints. *Int J Adv Manuf Technol* 94:1759–1770. <https://doi.org/10.1007/s00170-017-0043-5>
 6. Mostafapour A, Asad FT (2016) Investigations on joining of Nylon 6 plates via novel method of heat assisted friction stir welding to find the optimum process parameters. *Sci Technol Weld Join* 21:660–669. <https://doi.org/10.1080/13621718.2016.1169669>
 7. Hoseinlghab S, Mirjavadi SS, Sadeghian N et al (2015) Influences of welding parameters on the quality and creep properties of friction stir welded polyethylene plates. *Mater Des* 67:369–378. <https://doi.org/10.1016/j.matdes.2014.11.039>
 8. Aghajani H, Simchi A (2018) Experimental and thermomechanical analysis of the effect of tool pin profile on the friction stir welding of poly (methyl methacrylate) sheets. *J Manuf Process* 34:412–423. <https://doi.org/10.1016/j.jmapro.2018.06.015>
 9. Panneerselvam K, Lenin K (2014) Joining of Nylon 6 plate by friction stir welding process using threaded pin profile. *J Mater* 53:302–307. <https://doi.org/10.1016/j.matdes.2013.07.017>
 10. Nath RK, Barma JD, Singh N (2019) An experimental investigation of the effect of tool rotational speed on the force, torque and mechanical behaviour of friction stir welded PVC sheets. *IOP Conf Ser Mater Sci Eng*. <https://doi.org/10.1088/1757-899X/577/1/012108>
 11. Mendes N, Neto P, Simão MA et al (2016) A novel friction stir welding robotic platform: welding polymeric materials. *Int J Adv Manuf Technol* 85:37–46. <https://doi.org/10.1007/s00170-014-6024-z>
 12. Aghajani Derazkola H, Simchi A, Lambiasi F (2019) Friction stir welding of polycarbonate lap joints: relationship between processing parameters and mechanical properties. *Polym Test* 79:105999. <https://doi.org/10.1016/j.polymertesting.2019.105999>
 13. Scialpi A, Troughton M, Andrews S, de Filippis LAC (2009) Viblade™: friction stir welding for plastics. *Weld Int* 23:846–855. <https://doi.org/10.1080/09507110902843271>
 14. Bagheri A, Azdast T, Doniavi A (2013) An experimental study on mechanical properties of friction stir welded ABS sheets. *Mater Des* 43:402–409. <https://doi.org/10.1016/j.matdes.2012.06.059>
 15. Banjare PN, Sahlot P, Arora A (2017) An assisted heating tool design for FSW of thermoplastics. *J Mater Process Technol* 239:83–91. <https://doi.org/10.1016/j.jmatprotec.2016.07.035>
 16. Mendes N, Loureiro A, Martins C et al (2014) Morphology and strength of acrylonitrile butadiene styrene welds performed by robotic friction stir welding. *Mater Des* 64:81–90. <https://doi.org/10.1016/j.matdes.2014.07.047>
 17. Azarsa E, Mostafapour A (2014) Experimental investigation on flexural behavior of friction stir welded high density polyethylene sheets. *J Manuf Process* 16:149–155. <https://doi.org/10.1016/j.jmapro.2013.12.003>
 18. Pirizadeh M, Azdast T, Ahmadi SR, Mamaghani S (2013) Friction stir welding of thermoplastics using a newly designed tool. *J Mater*. <https://doi.org/10.1016/j.matdes.2013.08.053>
 19. Vijendra B, Sharma A (2015) Induction heated tool assisted friction-stir welding (i-FSW): a novel hybrid process for joining of thermoplastics. *J Manuf Process* 20:234–244. <https://doi.org/10.1016/j.jmapro.2015.07.005>
 20. Eslami S, Ramos T, Tavares PJ, Moreira PMGP (2015) Shoulder design developments for FSW lap joints of dissimilar polymers. *J Manuf Process* 20:15–23. <https://doi.org/10.1016/j.jmapro.2015.09.013>
 21. Moochani A, Omidvar H, Ghaffarian SR, Goushegir SM (2019) Friction stir welding of thermoplastics with a new heat-assisted tool design: mechanical properties and microstructure. *Weld World* 63:181–190. <https://doi.org/10.1007/s40194-018-00677-x>
 22. Swolfs Y, Shi J, Meerten Y et al (2015) The importance of bonding in intralayer carbon fibre/self-reinforced polypropylene hybrid composites. *Compos Part A Appl Sci Manuf* 76:299–308. <https://doi.org/10.1016/j.compositesa.2015.06.017>
 23. Schmidt A, Taylor D (2021) Erosion of soft tissue by polypropylene mesh products. *J Mech Behav Biomed Mater* 115:104281. <https://doi.org/10.1016/j.jmbbm.2020.104281>
 24. Bahl S, Bagha AK, Sehgal S (2021) Experimental investigations into sound transmission loss by different materials at aircraft noise. *Mater Today Proc* 44:2048–2053. <https://doi.org/10.1016/j.matpr.2020.12.153>
 25. Nath RK, Maji P, Barma JDEB (2021) Joining of advance engineering thermoplastic using novel self-heated FSW tool. *JOM*. <https://doi.org/10.1007/s11837-021-04686-y>
 26. ASTM-E2015-04 (2006) Standard guide for preparation of plastics and polymeric specimens for microstructural examination. In: ASTM International, West Conshohocken, PA
 27. ASTM International (2016) Standard practice for preparation of metallographic specimens. *ASTM Int* 82:1–15. <https://doi.org/10.1520/D0638-14.1>
 28. ASTM International (2002) Standard test methods for flexural properties of unreinforced and reinforced plastics and electrical insulating materials D790. In: *Annu B ASTM Stand*, pp 1–12
 29. Nieh JY, Lee LJ (1998) Hot plate welding of polypropylene. Part I: crystallization kinetics. *Polym Eng Sci* 38:1121–1132. <https://doi.org/10.1002/pen.10279>
 30. Nath RK, Jha V, Maji P, Barma JD (2021) A novel double-side welding approach for friction stir welding of polypropylene plate. *Int J Adv Manuf Technol*. <https://doi.org/10.1007/s00170-021-06602-9>
 31. Elyasi M, Derazkola HA (2018) Experimental and thermo-mechanical study on FSW of PMMA polymer T-joint. *Int J Adv Manuf Technol* 97:1445–1456. <https://doi.org/10.1007/s00170-018-1847-7>
 32. Inaniwa S, Kurabe Y, Miyashita Y, Hori H (2013) Application of friction stir welding for several plastic materials. Woodhead Publishing Limited, New York
 33. Bambang K, Soenoko R, Purnowidodo A, Irawan YS (2020) Effect of friction stir welding process on crystallinity and degradation of polypropylene. *J Southwest Jiaotong Univ* 55:2
 34. Lambiasi F, Grossi V, Paoletti A (2019) Advanced mechanical characterization of friction stir welds made on polycarbonate. *Int J Adv Manuf Technol* 104:2089–2102. <https://doi.org/10.1007/s00170-019-04006-4>
 35. Moreno-Moreno M, Macea Romero Y, Rodríguez Zambrano H et al (2018) Mechanical and thermal properties of friction-stir welded joints of high density polyethylene using a non-rotational shoulder tool. *Int J Adv Manuf Technol* 97:2489–2499. <https://doi.org/10.1007/s00170-018-2102-y>

Publisher's Note Springer Nature remains neutral with regard to jurisdictional claims in published maps and institutional affiliations.